Title: Disease Modifying Osteoarthritis Drug Discovery Using A Temporal Phenotypic Reporter In Primary Human Chondrocytes

Authors: Maria A. Cruz[1], Makan Karimzadeh[1], Kari Martyniak[1], Ramapaada Medam[1], Thomas J. Kean[1*]

* Corresponding Author. Email: Thomas.Kean@ucf.edu

Affiliations:[1]Biionix Cluster, Internal Medicine, University of Central Florida College of Medicine; Orlando, FL 32827, USA.

One Sentence Summary: A novel drug (aromoline) and target receptor (dopamine receptor D4) were identified as stimulating type II collagen, with the goal to treat or prevent osteoarthritis.

Abstract: Osteoarthritis is a significant and growing problem with no disease modifying drugs in the clinic. Current screening platforms typically use 2D culture, immortalized or non-human cells in a hyperoxic environment. To challenge this paradigm and identify new drugs, we engineered primary human chondrocytes with a secreted luciferase reporter under the control of the articular cartilage marker, type II collagen. We then successfully screened a natural product library using a high throughput model with COL2A1-Gaussia luciferase primary human chondrocyte reporter cells in 3D aggregates under physioxia. We identified several candidate compounds that increased type II collagen over controls, with aromoline being the best candidate. Aromoline is a bisbenzylisoquinoline alkaloid that has been studied for its anti-proliferative, anti-inflammatory, and anti-microbial properties, and we are the first to explore its effects on chondrocytes and chondrogenesis. In silico analysis provided an unexpected initial candidate target protein: the dopamine receptor D4 (DRD4). The researchers confirmed upregulation in the expression of DRD4 and type II collagen after treatment with aromoline. This novel approach provides a platform for drug discovery in a challenging and under-researched area.

Main Text:

INTRODUCTION

Osteoarthritis (OA) is the most prevalent articular joint disease worldwide. It affects approximately 16% of adult in the US, with approximately 32.5 million adults reporting OA between 2008 to 2014 (*1*). Post-traumatic osteoarthritis (PTOA) is thought to account for up to 12% of cases (*2*). Current pharmaceutical therapies for OA are primarily palliative including non-steroidal anti-inflammatories, opioid analgesics, intra-articular corticosteroids and hyaluronan injections (*3*). Surgical intervention is the only current treatment that can restore at least partial function to the joint, however results are highly variable (*4*). There are currently no disease-modifying drugs available to treat OA, as such there is a dire need to identify novel regenerative pharmaceutical alternatives (*3*).

Cartilage degeneration is the primary pathological feature of osteoarthritis. Cartilage is composed of a dense extracellular matrix interspersed with chondrocytes. Chondrocytes synthesize a combination of glycosaminoglycans (GAG), proteoglycans and collagens that make up native cartilage. Type II collagen makes up 90-95% of all collagens found in articular

cartilage, and its degradation is one of the early symptoms of OA (*5-7*). Furthermore advances in tissue engineering for the treatment of OA and post traumatic osteoarthritis (PTOA) have been hampered by the inability to recapitulate native levels of type II collagen *in vitro* (*8*). Previous work by our group has shown that increased type II collagen synthesis correlates with improved mechanical and biochemical properties in engineered tissue *in vitro* (*9-11*). In this study we propose using type II collagen expression as a chondrogenic phenotype for drug discovery.

Traditional methods to measure type II collagen, such as biochemical assays, protein assays, and real time qPCR are laborious, costly, time consuming, and destructive to samples (*12*). We have developed a phenotypic COL2A1-*Gaussia* luciferase primary human chondrocyte reporter (HuCol2gLuc) that allows for non-destructive temporal analysis of type II collagen production (*13*). In this work, the modified chondrocytes are used in a 3D aggregate model enabled for high throughput analysis. Published findings by our group have shown the success of this assay, by using it to identify vitamins and minerals that improve chondrogenesis in the murine chondrogenic cell line, ATDC5, and in primary rabbit chondrocytes (*10, 14*). This system has also been used to identify biomaterials that improve type II collagen production in human primary chondrocytes in 3D bioprinted constructs (*13*). In this study we used the phenotypic reporter system to identify new lead compounds, that can stimulate type II collagen production in primary human chondrocytes by screening the NCI natural products Set V library (*15*).

Natural Products are great source of potential new drugs and lead compounds. This class of compounds have large structural diversity and are enriched in bioactive compounds covering a wider chemical space compared to chemically synthesized compounds (*16, 17*). They have been a prolific source of leads in drug discovery, with several marketed drugs being or having been modified from natural products (*18, 19*). Despite their advantages, isolation, and characterization of natural products from their original source, followed by lack of high throughput methodologies to screen natural products, are primary drawbacks that have hampered natural product advancement in drug discovery (*20, 21*).

Using our 3D *in vitro* phenotypic reporter assay we have successfully screened the Natural Product Set V library from NCI. This library consists of 390 compounds selected from the 140,000 products from the DTP Open Repository collection. Compounds for this library were selected based on origin, purity (>90% by ELSD, major peak has correct mass ion), structural diversity and availability of compound. From the screen we have identified a hit for increased type II collagen production. Furthermore, we have identified a potential target for OA drug discovery.

RESULTS

Initial screen of natural products library identified two hits that increased type II collagen synthesis in vitro

To screen 390 natural products from the NCI natural products library, primary human chondrocytes were modified to express a *Gaussia* luciferase secreted reporter driven by type II collagen promoter. HuCol2gLuc primary human chondrocytes have been previously characterized by our group as retaining chondrogenic capacity and luminescence serving as a proxy for type II collagen expression (*13*). Aggregate cultures of HuCol2gLuc cells were seeded in the presence of the 390 compounds from the library continuously over 22 days in defined chondrogenic differentiation medium with feedings every 2-3 days (*22, 23*). **Figure 1A** shows overall results of treatment. Of the 390 compounds, 77 were cytotoxic to cells. These were

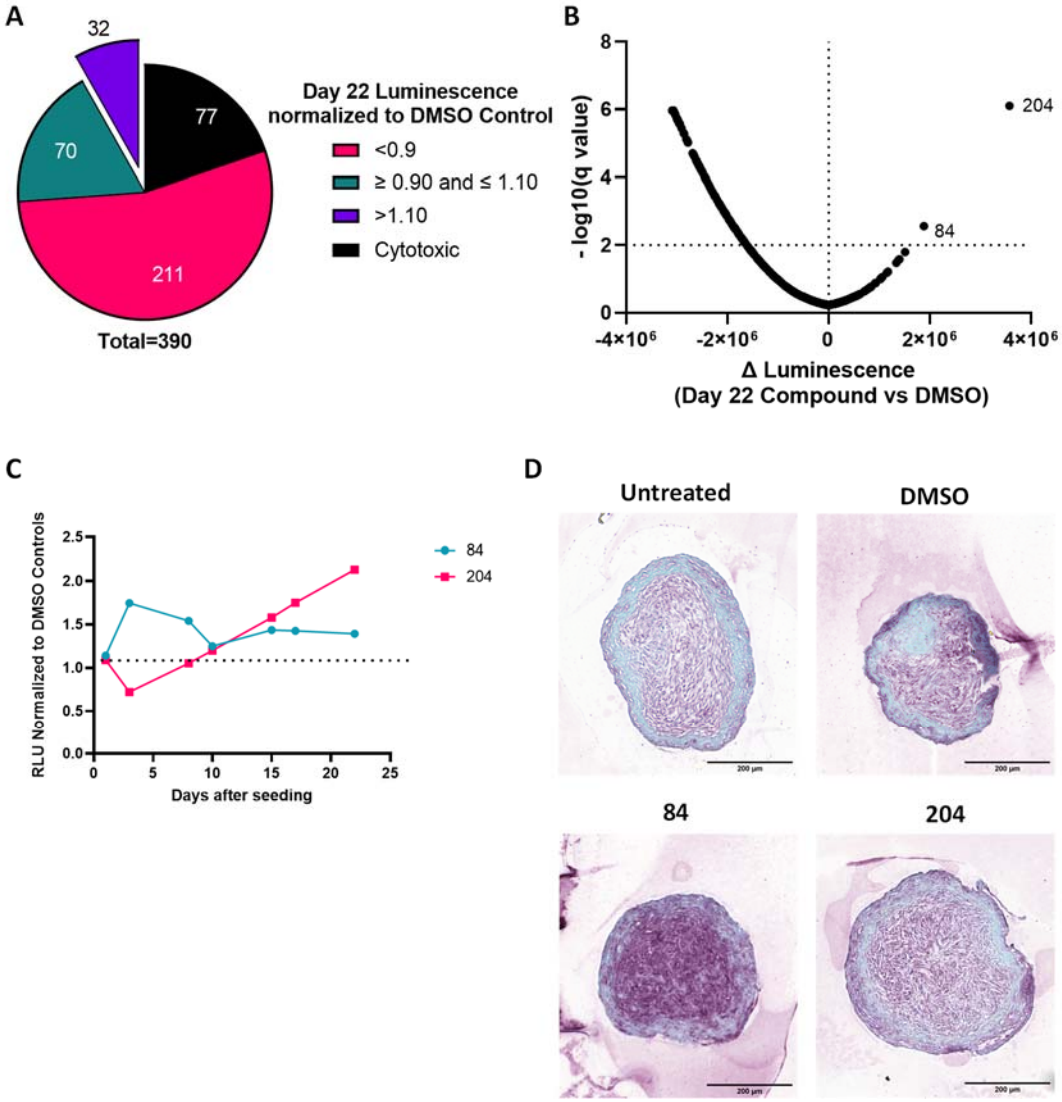

Fig. 1. Drug Screen of natural product library via HuCol2gLuc system identified hits that increased type II collagen

(**A**) Overview of Day 22 luminescence for 390 Natural Drug Screen Library normalized to DMSO (vehicle) control. (**B**) Volcano Plot of day 22 aggregate luminescence vs. DMSO control. (**C**) Temporal luminescence signal of aggregates treated with candidates 84 (aromoline) and 204 (deserpidine) over 22 days with results normalized to DMSO control. (**D**) Immunohistological staining for type II collagen of day 22 aggregates treated with candidate 84, 204 and controls for type II collagen. Scale Bars = 200 µm.

identified as a failure to form aggregates after initial treatment. Of those that were not cytotoxic 211 compounds were detrimental to chondrogenesis, classified as less than 90% of vehicle (DMSO) control aggregate luminescence on day 22 (**Fig. 1A**). We identified 70 compounds had little effect on type II collagen expression (90-110% of luminescence) and 32 compounds were considered beneficial (>110% of control). Of those 32, only two candidates, identified as 84 (aromoline) and 204 (deserpidine), had a significant increase in luminescence as compared to the controls by day 22, shown by the volcano plot in **Fig 1B.** Luminescence over 22 days normalized to our DMSO control is shown in **Fig 1C**. The overall trend of expression for both candidates differs over the 22 days. As seen in **Fig 1C** aggregate sample treated with aromoline shows an

increase over the control as early as day 3 with a sustained increase in expression over 22 days. Alternatively, luminescence of aggregate treated with deserpidine shows an initial decrease in expression with continued increase in luminescence after day 8. Immunohistochemistry of sections collected from aggregates at day 22 shown in **Fig 1D** confirm expression of type II collagen in HuCol2gLuc derived aggregates with substantially darker staining in the aggregate treated with aromoline.

Validation of hits from the screen in two different cell donors verified aromoline as a hit

To validate aromoline and deserpidine from the drug screen, HuCol2gLuc cells, from two different donors, were treated with either aromoline or deserpidine in aggregate culture for 22 days in chondrogenic differentiation medium supplemented with 10ng/ml of TGF-β1. As seen in **Fig 2A** and **2C**, deserpidine treatment resulted in an increase in luminescence in aggregates from donor 1 cells but not donor 2. Luminescence for deserpidine in donor 1 aggregates decreased from day 0 to day 10 with a significant increase from day 15 to day 22, similar to what was observed in the initial drug screen. In contrast, aromoline resulted in increased luminescence for donor 2 both cumulatively and on days 8 and 10, shown in **Fig 2C** and **Fig 2D,** but only at day 3 for donor 1, shown in **Fig 2A**. The increase in luminescence for donor 2 aggregates treated with

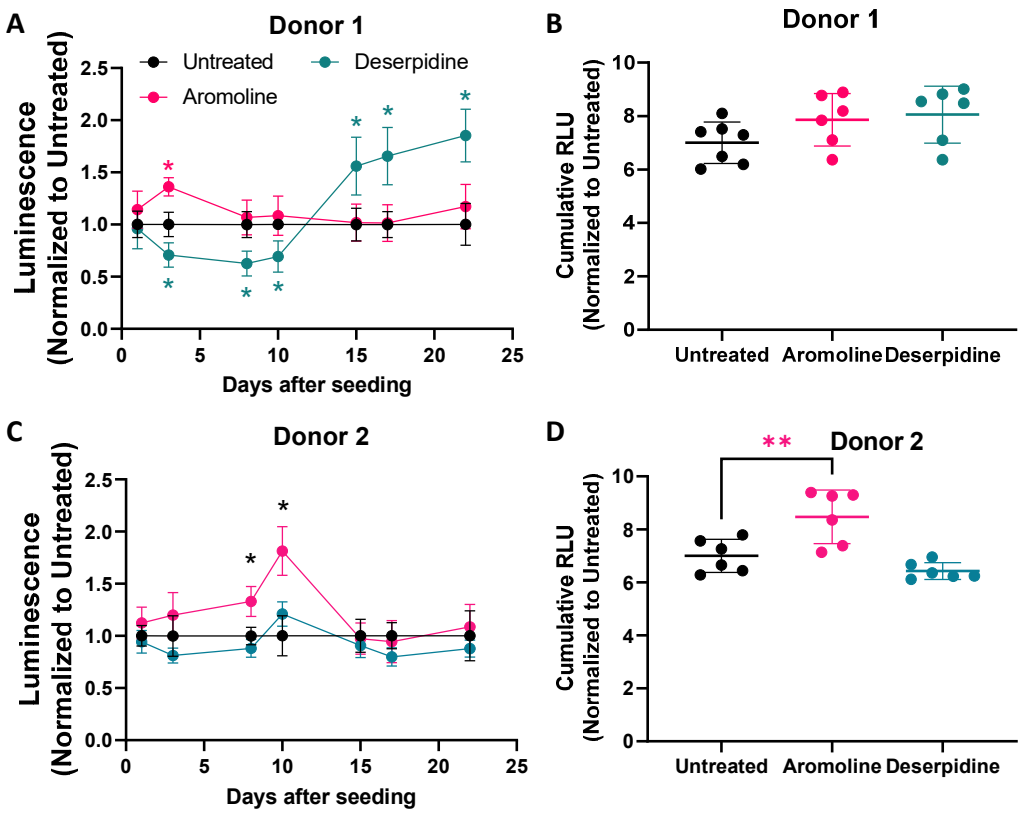

Fig. 2. Validation of hits confirmed increased type II collagen expression with aromoline treatment
Drug Candidates selected from the screen were tested in aggregate culture of HuCol2gLuc reporter human chondrocytes from two different donors. Results are shown as luminescence over 22 days normalized to an untreated control, for donor 1 (**A**) and donor 2 (**B**). Results are also presented as cumulative luminescence signal for donor 1 (**C**) and donor 2 (**D**). N = 6. Individual replicates or mean of replicates are shown with error bars indicating standard deviation and * indicating p <0.01 vs. untreated control. * aromoline; * deserpidine.

aromoline compared to the untreated control occurred from day 0 to day 10 with no change from day 15 to day 22, as compared to the control (**Fig 2C**).

This is also similar to the initial screen, where aromoline had a peak in luminescence early in chondrogenesis versus late. Contrary to **Fig 2A**, deserpidine showed no significant increase in donor 1 for cumulative luminescence. As seen in **Fig 2D**, aromoline showed a significant increase in cumulative luminescence for donor 2 with a positive trend for donor 1.

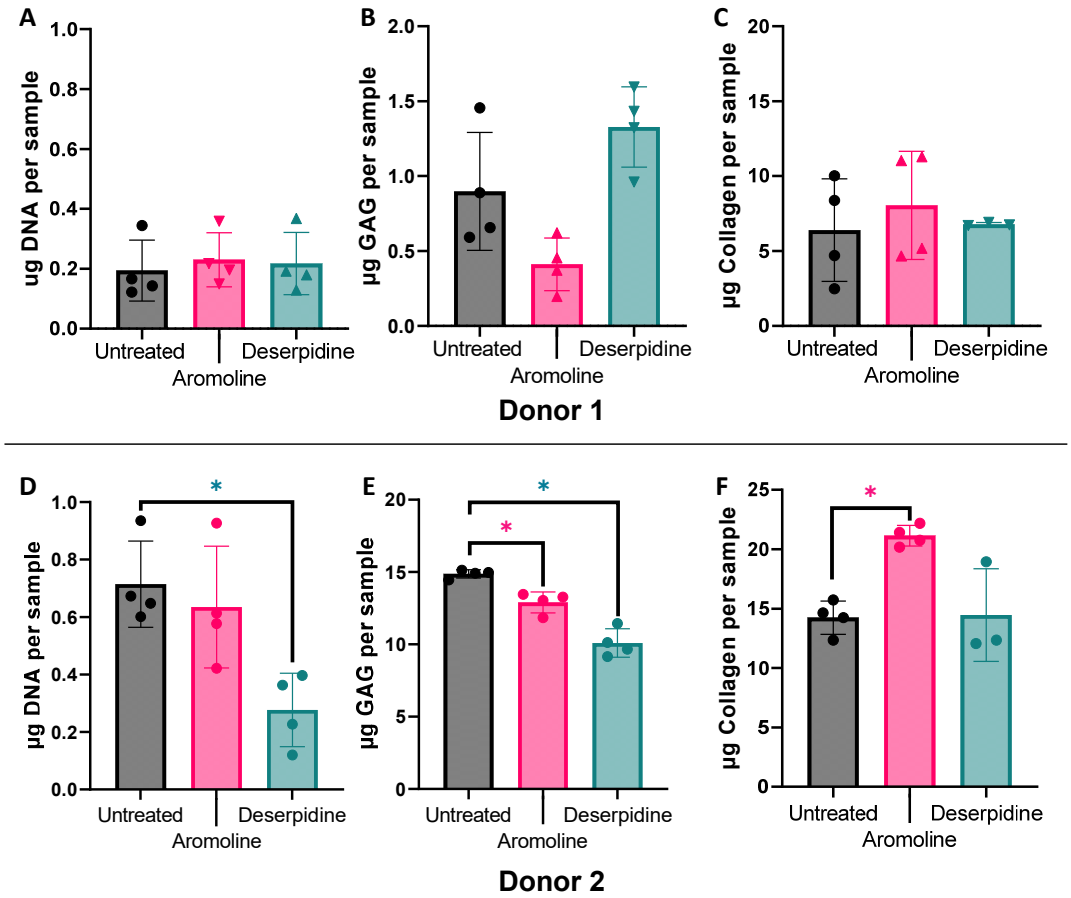

Fig. 3. Biochemical assays on HuCol2gLuc aggregates from two donors at day 22
Total DNA content for donor 1 (µg per sample) is shown in (**A**) and for donor 2 in (**D**). Glycosaminoglycan content was quantified in (**B**) for donor 1 and (**E**) for donor 2. Total of micrograms of collagen content for donor 1 and donor 2 are shown in (**C**) and (**F**) respectively. N = 4. Individual replicates or mean of replicates are shown with error bars indicating standard deviation and * indicating p <0.01 vs. untreated control, * aromoline; * deserpidine.

To corroborate luminescence results, biochemical assays to quantitate DNA, glycosaminoglycan (GAG) and total collagen content were performed at the end of culture (day 22). **Fig. 3A and 3D** shows an average of ~0.2 µg of DNA per donor 1 samples and ~0.7 µg per donor 2 samples. There is no significant difference between drug treatments for donor 1. Treatment with aromoline also had no change in DNA content for donor 2, however treatment with deserpidine showed a significant decrease in DNA content compared to the untreated control (**Fig. 3D**). This

suggests that aromoline has no effect on cell proliferation or viability over 22 days, while deserpidine seems to have a donor dependent effect on cell viability. Total glycosaminoglycan content is shown in **Fig. 3B and 3E**. There seems to be a decrease in GAG content with aromoline in donor 1 and 2 aggregates, although donor 1 results were not statistically significant. Deserpidine treatment had no effect on GAG for donor 1 but had a significant decrease in donor 2 to 10 μg vs. 15 μg in the untreated controls, corroborating the donor dependent effects of deserpidine. Quantification of total collagen, as seen in **Fig. 3C and F** shows no significant increase in total collagen with deserpidine treatment in either donor 1 or donor 2 aggregates vs. untreated control. Treatment with aromoline resulted in a significant increase in donor 2 aggregate collagen, to ~21 μg over untreated (~14μg), and a positive upward trend in donor 1. Furthermore, a substantial difference in the total DNA, GAG, and collagen content was noted between donor 1 and donor 2 regardless of treatment. Altogether aggregates from donor 1 cells seem to be less chondrogenic than aggregates from donor 2. Based on cumulative luminescence in donor 2 and total collagen content, aromoline was identified as a top hit for the stimulation of type II collagen.

Aromoline has a dose dependent effect on HuCol2gLuc aggregate type II collagen expression

To characterize the response of HuCol2gLuc cells, to treatment with aromoline, cells were cultured in 3D aggregates in chondrogenic media treated with different concentrations of aromoline (0-10 μM). Dose response curves were generated from luminescence data at day 3 (**Fig. 4A**), day 10 (**Fig. 4B**) and for cumulative luminescence (**Fig. 4C**). As seen in Figure 4, there was a dose dependent increase in type II collagen driven-luminescence with a calculated 50% effective concentration (EC50) of 2.46 μM, 2.58 μM, and 3.07 μM for day 3, 10 and cumulative luminescence respectively. To determine effects of aromoline on viability and cell proliferation, resazurin assay and quantification of DNA content were carried out at day 22. **Fig. 4D** shows that there is a dose dependent decrease in resazurin fluorescence at day 22 suggestive of decreased metabolic activity due to aromoline treatment. DNA quantification shows a similar trend with a significant decrease in aggregates treated with 10 μM aromoline (**Fig. 4E**). This suggests that decreased metabolic activity is due to cytotoxicity at 10 μM aromoline. Immunohistochemistry of sections collected from aggregates at day 22 shown in **Fig. 4F-4I** confirm expression of type II collagen in HuCol2gLuc derived aggregates with no notable differences between aggregates treated with these doses of aromoline.

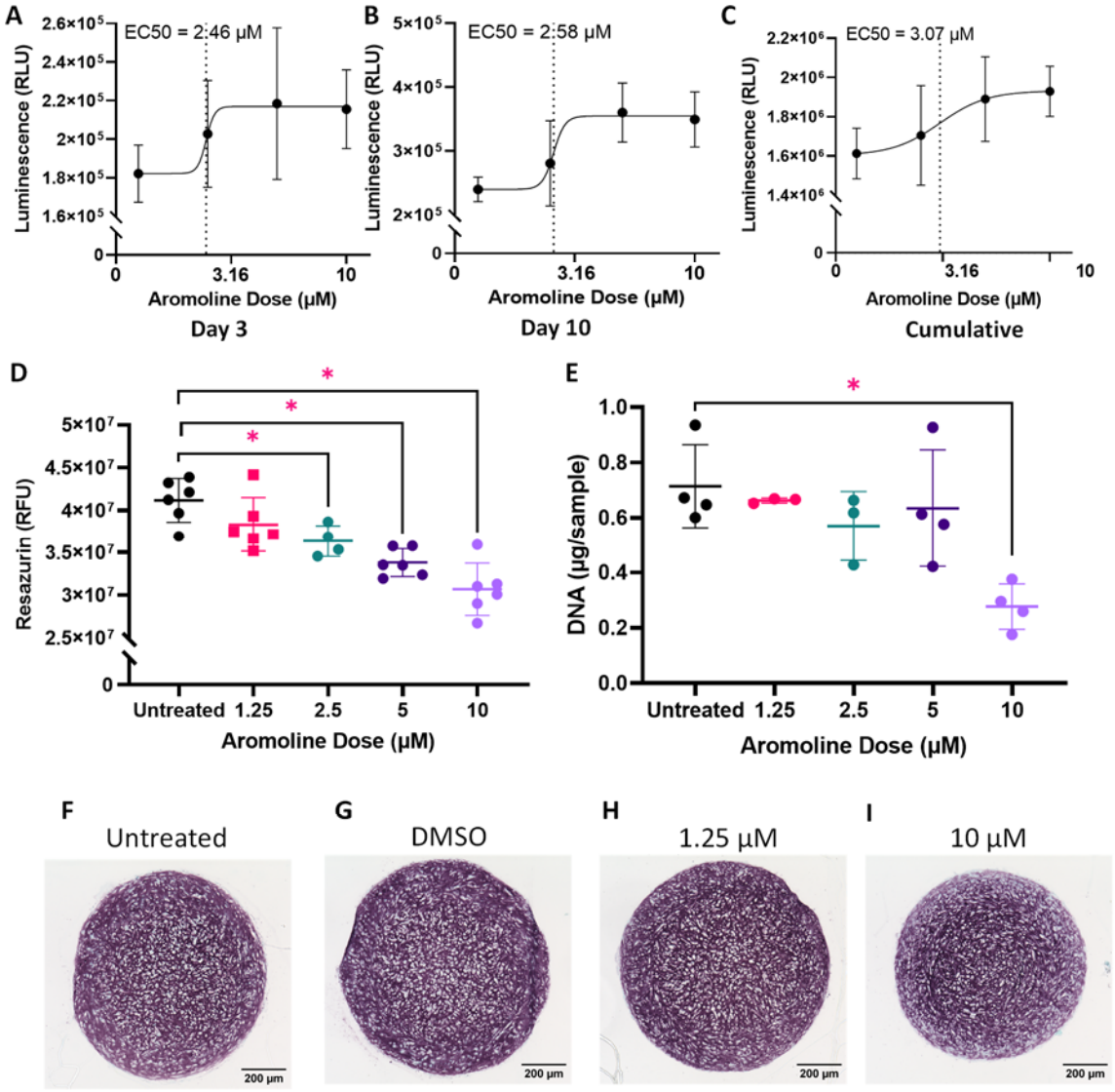

Fig.4. Response of HuCol2gLuc aggregates to aromoline is dose dependent

HuCol2gLuc aggregates were treated with aromoline (0-10 µM). Dose response curves were generated from luminescence data at day 3 (**A**), day 10 (**B**) and cumulative luminescence over 22 days (**C**). Metabolic activity (**D**) and DNA content (**E**) are shown at day 22. N= 6. Individual replicates or mean of replicates are shown with error bars indicating standard deviation and * indicating $p < 0.05$ vs. untreated control. Type II collagen staining of day 22 aggregates treated with indicated doses of aromoline (**F-I**). Scale Bars = 200 µm.

Characterization and target identification of aromoline

We attempted to identify potential targets for aromoline, by using its chemical structure **(Fig. 5A)** for *in silico* analysis via SwissADME and SwissTargetPrediction (*24-26*). Using the Swiss target prediction tool, we determined that about 40% of the predicted targets are family A G-protein coupled receptors (**Fig. 5B**). By homology, the specific target with the highest probability was the Dopamine 2 receptor (*DRD2*). Interestingly, several of the other compounds from the screen also showed dopamine receptors as a target (Supplemental Data 1). Our previous work showed expression of only the dopamine 4 receptor (*DRD4*), a DRD2-like receptor, in human chondrocytes (*27*). Another study looking at mesenchymal stromal cell chondrogenesis, via RNA-Seq, also showed DRD4 as the only dopamine receptor expressed during chondrogenesis (**Fig. 5C**; (*28*)). Interestingly, expression of DRD4, shown in (**Fig. 5C**) increases during chondrogenesis with a peak at around week 2, similar to the type II collagen pattern observed for aggregates treated with aromoline (**Fig. 2C**). Furthermore, immunohistochemistry confirmed the expression of DRD4 in tissue engineered human cartilage (**Fig. 5D**), with a different more punctate pattern of staining as compared to DRD4 staining in the mouse brain where dopamine receptors are widely expressed.

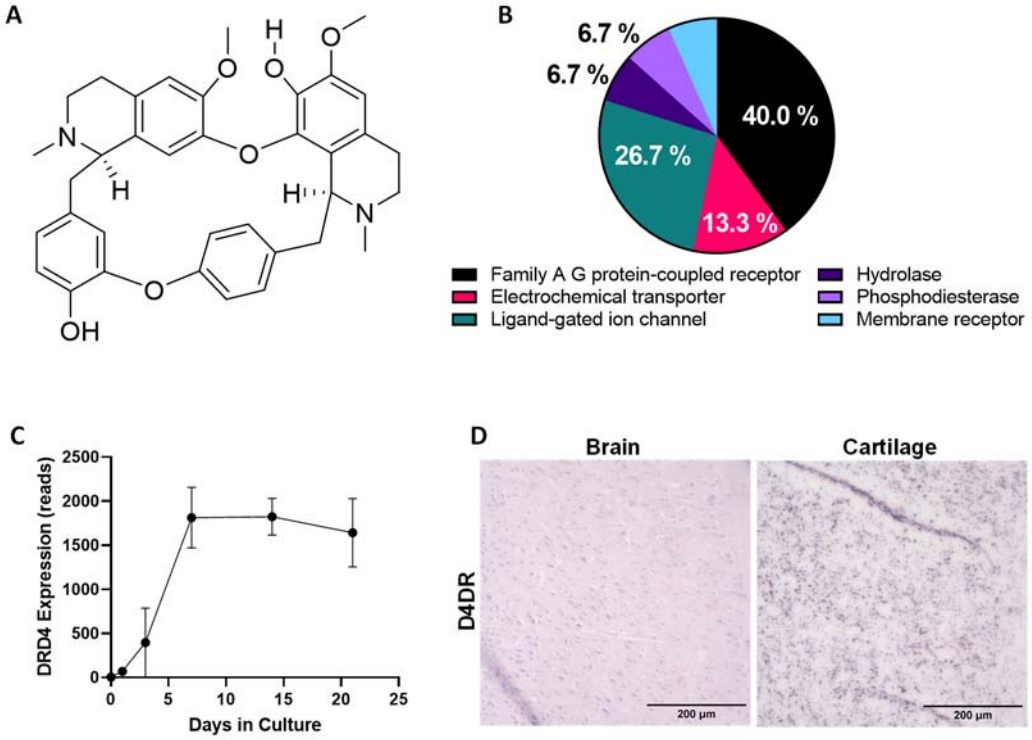

Fig.5. Structure and predicted targets for aromoline

Chemical structure of aromoline (**A**). SwissTargetPrediction predicted targets for aromoline presented by target class (**B**). DRD4 temporal expression in human mesenchymal stromal cells (MSCs) during 21 days of chondrogenesis ((28) **C**, n = 3). DRD4 staining (purple) in mouse brain and in tissue engineered human cartilage (**D**) Scale Bars = 200 µm.

DRD4 selective antagonist and agonists have a dose dependent effect on HuCol2gLuc aggregate type II collagen expression

To determine whether DRD4 signaling affected type II collagen expression in human chondrocytes, HuCol2gLuc cells from donor 2 were cultured in 3D aggregates in the presence of a selective DRD4 agonist (ABT 724) or antagonist (PNU 96415E) at various concentrations (0-25 μM) and luminescence assessed over 22 days. As seen in **Fig. 6A**, ABT 724 treatment resulted in an increase in luminescence at day 8 at 10 μM and 25 μM concentrations with a sustained signal until day 22. ABT 724 had no effect at 0.1 μM or 1 μM. Cumulative luminescence (**Fig. 6B**) corroborates the results with concentrations of 10 μM and 25 μM resulting in a significant increase in luminescence as compared to the untreated controls. Unexpectedly, treatment with antagonist, PNU 96415E (**Fig. 6C** and **6D**) also had a positive effect on type II collagen-driven luciferase expression with the higher concentrations, 12.5 μM and 25 μM, resulting in increased luminescence compared to the untreated controls. The pattern of expression over 22 days, seen in **Fig. 6C**, differed from treatment with ABT 724 (**Fig. 6B**), with PNU 96415E treatment resulting in peak expression by day 10 followed by a decrease at day 15 and sustained expression until day 22. Cumulative luminescence (**Fig. 6D**) corroborates the results with concentrations of 12.5 μM and 25 μM resulting in a significant increase in luminescence as compared to the untreated controls. Immunohistochemistry confirmed the expression of type II collagen in aggregates treated with ABT 724 and PNU 96415E. ABT 724 had more intense staining for type II collagen as compared to the untreated control, while PNU 96415E had diminished type II collagen staining as compared to the control. DRD4 immunohistochemistry similarly shows a substantial increase in staining for aggregates treated with ABT 724 as compared to the control (**Fig. 6E**). Whereas PNU 96415E had similar staining as compared to the untreated control (**Fig. 6E**).

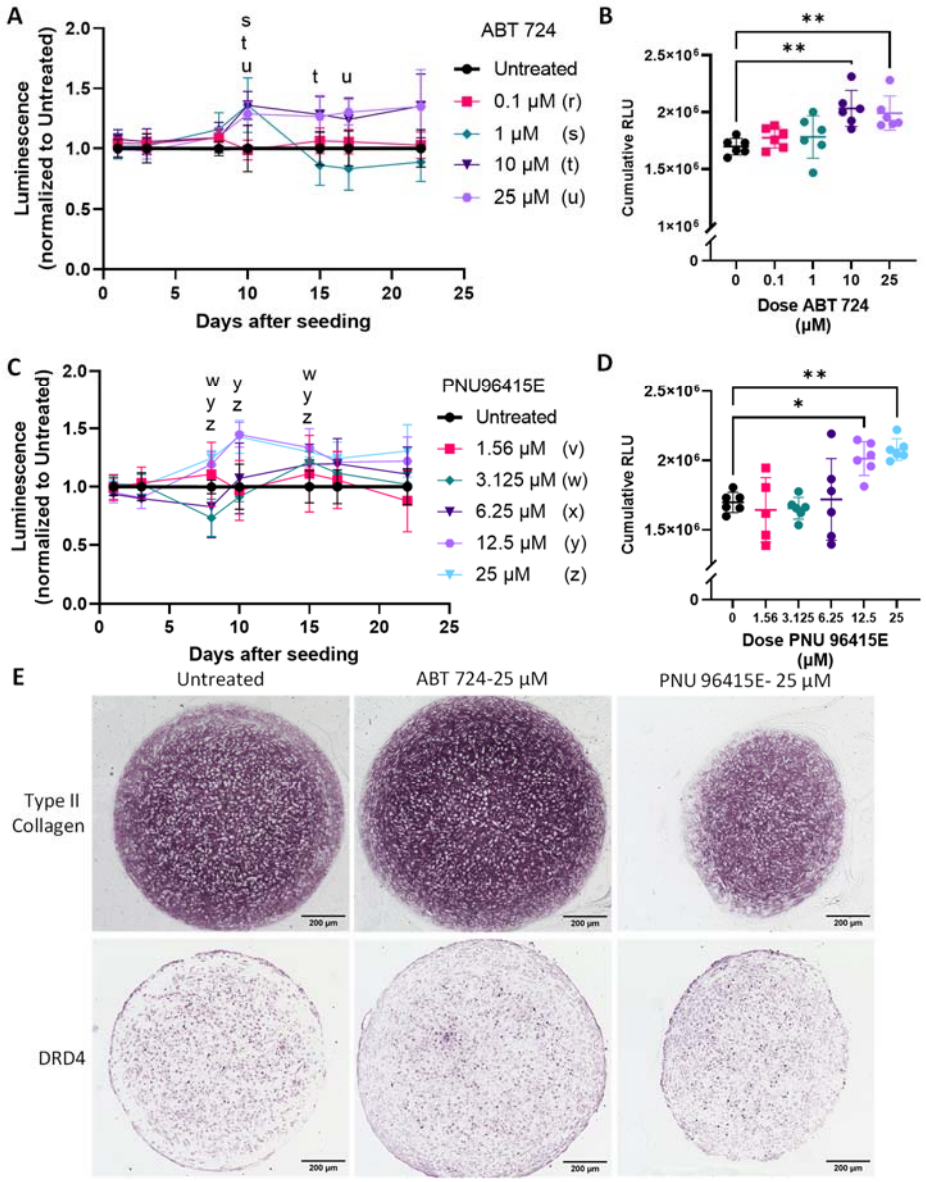

Fig. 6. DRD4 selective agonist and antagonist treatment increased type II collagen expression in HuCol2gLuc aggregates

Luminescence signal over 22 days after treatment with DRD4 agonist (ABT 724 (**A**)) and DRD4 antagonist (PNU 96415E (**B**)). Statistically significant differences vs. untreated control are indicated by the respective letters for the dose (s, t, u, w, y, z). Results also shown as cumulative luminescence for treatment with ABT 724 (**C**), and PNU96415E (**D**). N = 6. Individual replicates or mean of replicates are shown with error bars indicating standard deviation and * indicating p <0.05, and ** indicating p <0.01 vs. untreated control. Immunohistological staining for DRD4 and type II collagen in HuCol2gLuc aggregates after ABT 724 and PNU 96415E treatment at indicated doses (**E**). Scale Bars = 200μm.

To assess whether aromoline had an effect on DRD4 expression in human chondrocytes, monolayer culture of human chondrocytes from donor 1 and donor 2 were treated with drug aromoline (5μM) for 24 h followed by RNA extraction and analysis via qPCR. As seen in **Fig. 7A and 7B,** treatment with aromoline resulted in significant upregulation of DRD4 in both donor 1 and donor 2. Donor 1 had overall higher DRD4 expression as compared to the untreated

control, approximately 5-fold more, while donor 2 had only about 1.8-fold higher expression. Histology of donor 2 HuCol2gLuc aggregates treated with aromoline (10 μM) at day 22 shown in **Fig. 7C** confirm increased expression of DRD4 expression compared to untreated controls. To determine what signaling pathways could be involved in aromoline mediated increase of type II collagen, donor 2 primary chondrocytes were treated with aromoline in monolayer culture for 24 h, lysate collected, and a phospho-kinase array was used to look at levels of phosphorylation for 17 different kinases (**Fig. 7D**). Data normalized to reference spots and to DMSO controls is shown in **Fig. 7E.** There is a substantial decrease in AKT 1/2/3 phosphorylation at both T308 and S473 phosphorylation sites (**Fig.7E**). A less considerable decrease in p53 phosphorylation at the S15 site, in STAT3 phosphorylation at Y705, and in HSP 60 was also observed (**Fig. 7E**). Also observed was a modest increase in phosphorylation of CREB, EGFR, and eNOS (**Fig. 7E**).

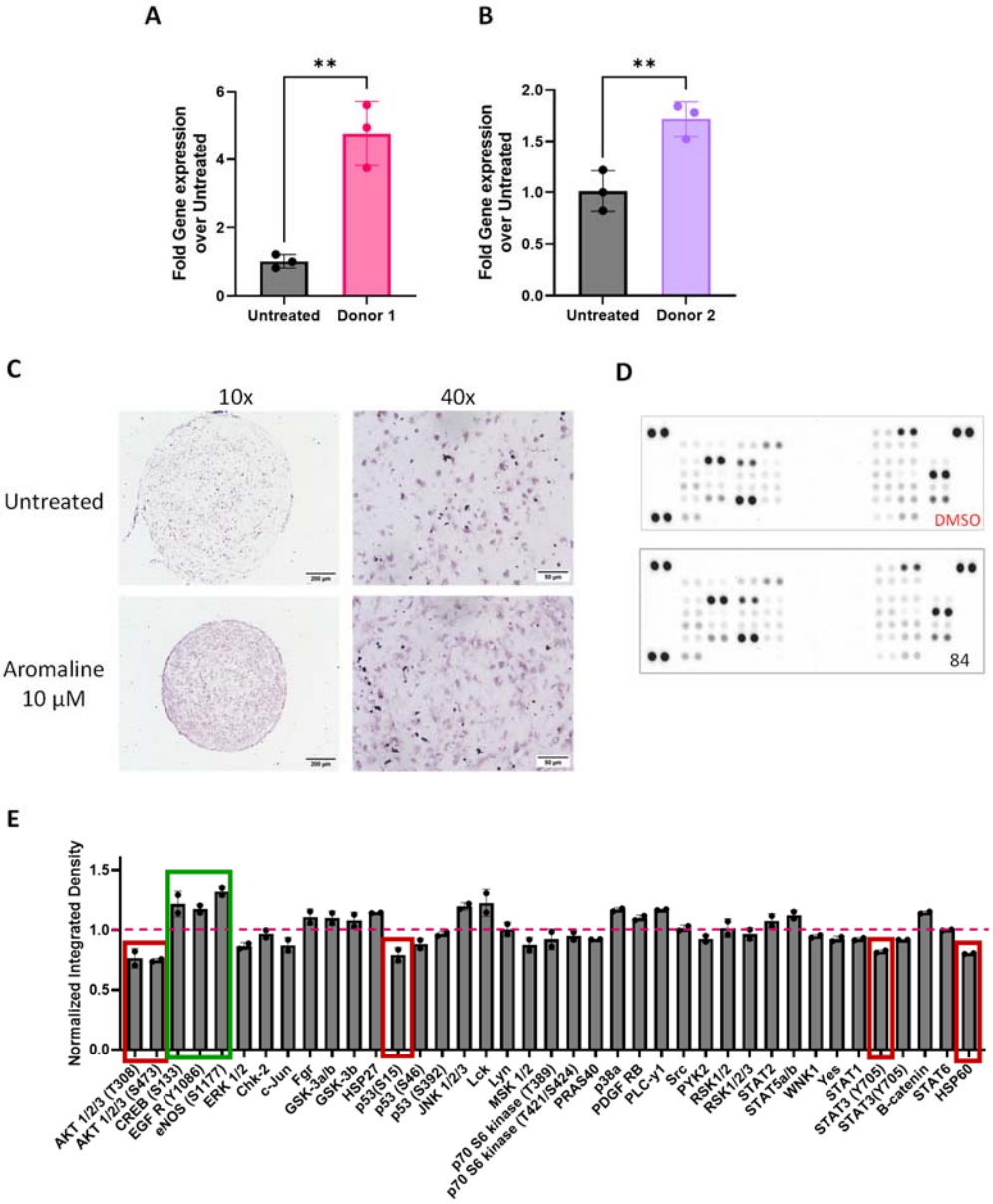

Fig. 7. Aromoline increases DRD4 expression in primary human chondrocytes
Expression of *DRD4* in monolayer cultures of primary human chondrocytes via PCR after treatment with aromoline for 24 hours. Show for donor 1 (**A**) and donor 2 (**B**) Results shown as fold changed vs. untreated control and normalized to reference gene *HPRT*. N = 3. Immunohistological staining (purple) for DRD4 in HuCol2gLuc aggregates after treatment with aromoline (**C**). Scale Bars = 200 µm. Dot blot of kinase phosphorylation of primary human chondrocytes after treatment with aromoline or DMSO as a vehicle control (**D**). Data from the dot blots is also shown as normalized integrated density (**E**). Error bars indicate standard deviation and ** indicate p <0.01.

DISCUSSION

Using our high throughput model of COL2A1-*Gaussia* luciferase primary human chondrocyte reporter (HuCol2gLuc) in 3D aggregates under physioxia we have successfully screened an NCI Natural product library. Our system has several advantages over other proposed models. It makes use of human primary cells over non-human cells or immortalized cell lines. While chondrocytes are generally limited in availability and could be a barrier for high throughput screening, our use of porcine derived synoviocyte matrix for expansion preserves chondrogenic capacity for more cell divisions and allowed for greater expansion of primary chondrocytes (*29, 30*). Our system tests compounds in 3D aggregates while other chondrogenic models for drug discovery typically rely on 2D culture (*31-33*). Two-dimensional culture for many cell types, including chondrocytes, fail to mimic cell to cell and cell to matrix interactions, as well as paracrine signaling events that are responsible for physiological tissue structure (*34, 35*). Furthermore, 2D culture cannot correctly model events, such as ECM sequestering of soluble compounds, which can have a large effect on drug - cell interactions (*35-37*). Overall 3D models better mimic native tissue. The primary advantage of our reporter model is the use of a secreted reporter which not only allows us to quantitate the signal as opposed to other read out methods such as staining and microscopy imaging but also allows for temporal non-destructive assessment of the phenotype during chondrogenesis (*10*).

From the natural product screen, we identified several candidate compounds that increased type II collagen over controls at one or more timepoints (Supplemental Data 1). Of these, aromoline and deserpidine had the most pronounced effect. In a follow up experiment aromoline presented as the better candidate while deserpidine had inconclusive results. Aromoline (NSC93674) is a bisbenzylisoquinoline alkaloid generally derived from members of the *Berberis* and *Stephania* genus (*38, 39*). As their name suggests, and as seen in **Fig. 5A,** these alkaloids consist of two benzylisoquinoline parts linked through either diphenyl ether, benzyl phenyl ether, or biphenyl bonds (*39, 40*). Previous screening of alkaloids from *Berberis* have shown that aromoline is a potent inhibitor of butyrylcholinesterase with low blood brain barrier permeability (*41*). However, neither our RNA-Seq data nor that of Huynh et al. showed expression of butyrylcholinesterase in chondrocytes or their progenitors (*27, 28*). Another study showed weak anti-microbial activity against *Plasmodium falciparum* with low cytotoxicity in the KB cell line (*42*). Although there is little published research on aromoline, various bisbenzylisoquinoline alkaloids are being studied for their anti-proliferative, anti-inflammatory and anti-microbial properties (*43-48*). This is the first study to our knowledge that explores the effects of aromoline on chondrocytes and chondrogenesis.

With so little known about the signaling pathways activated by aromoline, *in silico* analysis provided an unexpected initial candidate target: the dopamine 2 receptor. Dopamine receptors are G-coupled receptors widely expressed through the central nervous system (*49, 50*). Expression in the periphery has been observed in immune cells such as neutrophils, basophils, B cells and K cells, as well as the heart, kidneys, adrenal glands, blood vessels, and gastrointestinal tract (*51-59*). Dopamine receptors are classified under two groups the D1-like family that is coupled to G_s and activates adenylyl cyclase, and the D2-like family that is coupled to $G_{i\alpha}$ and inhibits adenyl cyclase (*60-62*). Based on the *in silico* target analysis, our previous RNA-seq and that of Huynh et al. (**Fig. 5C**), as well as the fact that dopamine receptors from the same family share significant homology, we hypothesized that Dopamine 4 Receptor (DRD4), one of the members of the D2-like receptors was a potential target for aromoline (*27, 28, 50*). This is the

first study to our knowledge that has highlighted the expression of DRD4, by RNA-Seq, qPCR and by immunohistochemistry, in primary human chondrocytes and cartilage. Furthermore, we confirmed upregulation in expression of DRD4 and type II collagen after treatment with aromoline (**Fig 7A-7D**).

Interestingly, treatment of HuCol2gLuc aggregates with either a selective agonist or antagonist for DRD4 resulted in increased type II collagen promoter-driven luminescence. However, the antagonist displayed a detrimental effect on pellet size, glycosaminoglycan content (**Supplemental Fig. 1**), and a decreased intensity in type II collagen histology staining (**Fig. 6E**). This suggests that the luminescence results for antagonist treatment are potentially false positives, a common and accepted aspect of screens, and highlight the importance of confirmation via alternative methods.

The best characterized pathway for extracellular matrix deposition by chondrocytes or their progenitors is that of transforming growth factor-beta superfamily and downstream effectors (*63-65*). In the non-canonical pathway, PI-3 kinase is stimulated, phosphorylating Akt which goes on to phosphorylate mTOR, resulting in metabolic changes including protein expression. Aromoline treatment in chondrocytes results in both upregulation of DRD4 expression and decrease in phosphorylation of Akt (**Fig. 7**), a distinct mode of action from both the canonical and non-canonical TGFβ pathways. A dopamine receptor $G_{i\alpha}$ independent pathway, the β-arrestin 2 pathway, could account for the observed effects of aromoline. The β-arrestin 2 pathway is activated as a mechanism for dopamine receptor internalization and desensitization (*66*). Formation of this complex results in inactivation of Akt by protein phosphatase 2 and activation of glycogen synthase kinase-3 (GSK3) signaling (*67*). GSK3 has been linked to maintenance of the chondrocyte phenotype. Inhibition of GSK3 results in cartilage destruction and progression of chondrocytes to terminal differentiation (*68-71*). Previous studies on dopamine receptors, as well as other GPCRs, have shown that ligand activation of β-arrestin 2 is distinct from its G protein dependent activity (*72-76*). Alternatively, the decrease in STAT3 phosphorylation and increase in CREB phosphorylation could be mechanisms for further research (*77*). These observations provide clues as to the mechanism of action for aromoline but fail to completely elucidate the pathways involved. As the production and deposition of extracellular matrix is both temporally and mechanistically distant from receptor activity, this is perhaps unsurprising. Further studies to unravel the signaling pathways involved in aromoline mediated type II collagen expression as well as DRD4 involvement in chondrogenesis are needed. Other areas of study include the identification of the endogenous ligand for DRD4 in chondrocytes and its role in chondrogenesis and osteoarthritis.

While a similar trend was evident with both donors, there was a significant difference in the extent of their response. This could be an interesting avenue for further, patient specific, tailored care. What is encouraging is the expression of DRD4 in cartilage in three separate studies: this research, the previous RNA-Seq data from our group (*27*) and in the work by Huynh et al. (*28*). There are multiple steps that need to be completed before translation to the clinic, confirmation in more donor chondrocytes, with non-modified chondrocytes and in an animal model(s).

This study not only provides novel insights into the complex process of chondrogenesis and extracellular matrix deposition but identifies a potential new target receptor and drug candidate for the anabolic treatment or prevention of osteoarthritis.

MATERIALS AND METHODS

To identify novel, chondrogenesis promoting drugs, human primary chondrocytes were genetically modified to express a secreted luciferase reporter under the control of the type II collagen promoter. Those cells were then used in a 3D culture system under physiological oxygen tension to screen a natural product library for promotion of the articular cartilage phenotypic marker, type II collagen. Identified compounds were further screened using in silico reference data to identify potential drug targets. The dopamine receptor D4 was identified and investigated as a potential target with significant effects on type II collagen expression.

Human primary chondrocyte isolation

Articular cartilage was isolated from visually intact areas of discarded surgical tissue as previously described (*13*). Tissue was collected from two donors during total joint re-placement surgery with informed consent under IRB approved protocols (Baylor College of Medicine, H-36683, H-36374). Discarded tissue (< 3h post-operation on ice in saline) was briefly stored in defined chondrogenic media (~4h, room temperature) before cartilage was dissected under sterile conditions. Isolated cartilage was diced into <1mm^3 pieces before digestion, first in hyaluronidase for 30 min (660 Units/ml Sigma, H3506; in DMEM/F12, 40ml), then by collagenase type II for ~16 hours at 37°C (583 Units/ml Worthington Biochemical Corp.; in DMEM/F12 with 10% FBS, 40ml). The digest was filtered through a 70 µm cell strainer, washed once with DMEM/F12, and resuspended in growth media (DMEM/F12 supplemented with 10% FBS (mesenchymal stromal cell selected (*78*)), 1% pen/strep). Cells were subsequently infected as described below or cryopreserved (95% FBS, 5% DMSO).

Lentiviral construct

Lentivirus was generated as previously described (*10, 13*). Briefly, custom COL2A1-*Gaussia* Luciferase plasmid (HPRM22364-LvPG02, GeneCopoeia, Inc.), envelope (pMD2.G) and packaging (psPAX2) plasmids were amplified in *Escherichia coli* (GCI-L3, GeneCopoeia) and purified via silica column (Qiagen Maxiprep) before co-transfection into HEK293Ta (GeneCopoeia) cells via calcium chloride precipitation. Newly packaged lentiviral particles were collected in culture medium after 48h and concentrated via ultracentrifugation (10,000 RCF, 4°C, overnight). Titers for COL2A1-Gluc lentivirus were estimated via real-time PCR and aliquots stored at -80°C.

Lentivirus infection of primary Human Chondrocytes

Isolated primary human chondrocytes, from each donor, were seeded at 6,100 cells/cm^2 in growth media (DMEM and allowed to adhere overnight (~20% confluency). Cells were infected with lentivirus (COL2A1-GLuc; MOI 25 in growth media) in the presence of 4 µg/ml polybrene (Opti-mem, Gibco) for 15 minutes at 4°C followed by overnight incubation at 37°C. Lentiviral medium was replaced with growth medium, and cells expanded to ~70-90% confluency. Cells were trypsinized (trypsin/EDTA 0.25%), then seeded on synoviocyte matrix coated flasks (*29*). Primary chondrocyte infection was done in physioxic (37°C, 5% O_2, 5% CO_2) conditions (*13, 79*). Newly generated COL2A1-GLuc cells were cryopreserved at the end of this first passage (95% FBS, 5% DMSO). These cells were used for all subsequent studies.

Chondrogenic Culture

Human COL2A1-GLuc or uninfected cells were thawed and seeded in growth media on synoviocyte matrix at 6,000 cells/cm^2 and expanded to 90-100% confluence in physioxia (*79, 80*). Cells were trypsinized (0.25% Trypsin/EDTA; Corning), resuspended in growth media (for monolayer culture) or chondrogenic differentiation media for 3D aggregates (93.24% High-Glucose DMEM (Gibco), 1% dexamethasone 10^{-5}M (Sigma), 1% ITS+premix (Becton-Dickinson), 1% Glutamax (Hyclone), 1% 100 mM Sodium Pyruvate (Hyclone), 1% MEM Non-Essential Amino Acids (Hyclone), 0.26% L-Ascorbic Acid Phosphate 50mM (Wako), 0.5% Fungizone (Life Technologies) with TGF-β1 (Peprotech) and seeded as described below.

Generation and Maintenance of 3D aggregates

To generate 3D aggregates, cells were seeded at 50,000 cells per well (in 96-well cell repellent u-bottom plates, GreinerBio) and then centrifuged at 500 RCF, 5 min. For the initial drug screen, aggregates were cultured in basal chondrogenic media (1ng/ml TGF-β1) alone, with DMSO (vehicle control) or 5 μM of the drug compounds from the NCI library (Natural Products V, NCI). For candidate validation and subsequent studies aggregates were cultured in basal chondrogenic media (10ng/ml TGF-β1) alone, with DMSO (vehicle control) or compounds as indicated in the results. DRD4 selective agonist ABT 724 and selective antagonist PNU 9641E were used at 1-25 μM based on prior literature (*81-83*). Aggregates were cultured for three weeks in physioxic conditions, culture medium was sampled and replaced three times a week with fresh medium. An OT-2 (Opentrons) python coded robotic pipette, programmed at an aspiration height of 2mm from the bottom of the wells and aspiration rate of 40 μl/s was utilized for addition of compound, cell feeding, and media sampling for luciferase assay (*13*). After three weeks, cell aggregates were either fixed in neutral buffered formalin for histology or medium removed and aggregates frozen (-20°C) for biochemical assays.

Luciferase Assay

Conditioned culture medium sampled from aggregates in 96-wells (20μL/well) was assessed using a stabilized *Gaussia* Luciferase buffer mix (50 μl/well) for a final concentration of 0.09 M MES, 0.15M Ascorbic Acid, and 4.2μM Coelenterazine in white 96-well plates. Luminescence was measured in a plate reader (25°C, relative light units (RLU), EnVision plate reader). An OT-2 (Opentrons) python coded robotic pipette was utilized for luciferase buffer addition to white plates (GreinerBio).

Metabolic Assay (Resazurin)

Metabolic activity was assessed on day 22 by adding resazurin (TCI chemicals) to a final concentration of 50 μM to each well and incubating at 37 °C in physioxia for 3 hours. After three hours, media (120 μl) was transferred to a 96-well black plate (Greinerbio) and fluorescence read at an excitation of 535nm and emission at 588nm. At OT-2 (Opentrons) python-coded robotic pipette was used to add resazurin to cell plates as well as to transfer medium to black plates.

Immunohistochemistry

At the end of three-week culture, aggregates were fixed in 10% Neutral Buffered Formalin overnight, and subsequently embedded in paraffin wax and sectioned (7µm sections). Sections were deparaffinized and hydrated, followed by treatment with pronase (1mg/ml, Sigma P5147, in PBS with 5mM $CaCl_2$) for epitope retrieval. Sections were blocked (BSA 3% w/v, Cohn Fraction V, Alfa Aesar) and incubated with mouse primary anti-Collagen Type II (DSHB II-II6B3) or mouse anti-dopamine 4 receptor (MABN125, Millipore) primary for 2 h at room temperature in a humidified chamber. II-II6B3 was deposited to the DSHB by Linsenmayer, T.F. (DSHB Hybridoma Product II-II6B3). Sections were then incubated with a biotinylated secondary (Vector Labs) followed Streptavidin-HRP (BD Biosciences). Sections were stained with a chromogen-based substrate kit (Vector labs, VIP substrate vector kit). All sections were imaged using a Keyence BZ-X810 microscope at 10x magnification.

Biochemical Assays

Aggregates frozen at day 22, were thawed with PBS, and digested with papain (25 µg/ml, Sigma, P4762, in 2mM cysteine; 50mM sodium phosphate; 2mM EDTA at a pH 6.5, 100 µl) at 65°C overnight (*13, 79, 84*). Plates were sealed with a qPCR adhesive sealing film (USA Scientific), a silicone sheet, and steel plates clamped to the plate to prevent evaporation during digestion. Half of the digest (50 µl) was transferred to another plate and frozen for hydroxyproline assessment. In the remaining digest, papain was inactivated with 0.1M sodium hydroxide (NaOH, 50 µl) followed by NaOH neutralization (100mM Na2HPO4, 0.1 N HCL, pH 1.82, 50 µl). To quantitate DNA content, samples of the neutralized digest (20 µl) were combined with buffered Hoechst dye (#33258, 667ng/ml, phosphate buffer pH 8, 100 µl) and fluorescence measured at an excitation of 365nm and emission of 460nm. For GAG assessment, 1,9-Dimethyl-methylene blue solution (195 µl) was added to neutralized digests (5 µl) and absorbance measured at 595nm and 525nm (*85*). Readings were corrected by subtracting 595nm reading from 525nm. Micrograms of DNA and GAG were calculated using a Calf thymus DNA standard (Sigma) or Chondroitin Sulfate standard (Seikagaku Corp.), respectively.

For hydroxyproline (HP) quantification, the frozen digests (50 µl) were thawed at room temperature and incubated overnight at 105°C with 6M hydrochloric acid (200 µl). Plates were sealed to prevent evaporation. Samples were then dried at 70°C overnight with a hydroxyproline standard (Sigma). Copper sulfate (0.15M, 10µl) and NaOH (2.5M, 10µl) were added to each well and incubated at 50°C for 5 minutes, followed by hydrogen peroxide (6%, 10 µl) for 10 minutes. Sulfuric acid (1.5 M, 40 µl) and Ehrlich's reagent (20 µl) were added, and samples incubated at 70°C for 15 minutes (*79*). Absorbance was measured at 505nm. Micrograms of hydroxyproline were calculated using the standard. Total collagen was calculated by the following formula (µg of HP X 7.6 = µg Total Collagen).

Reverse Transcription and Real-Time PCR

Primary human chondrocytes were seeded at 280,000 cells/well (12-well adherent plate, Corning) in growth media and allowed to adhere overnight. Growth media was replaced with chondrogenic media supplemented with 1ng/mL TGFβ1 alone or with aromoline. Cells were

treated for 24 h and then lysed and frozen. Lysate was thawed and RNA extraction and purification done following manufacturer's protocol (Ambion PureLink RNA Mini kit). RNA purity and integrity was assessed by RNA ScreenTape (Agilent Technologies) before use. cDNA was synthesized from 400ng RNA using a Maxima H Minus reverse transcriptase master mix following manufacturer's protocol. Quantitative real-time PCR for *DRD4* and *HPRT* (endogenous control) gene expression was done (qPCR) using SYBR green master mix (Applied Biosystems) and QuantStudio7 Flex Real-Time PCR system (ThermoFisher Scientific). Cycling parameters: 95°C for 20s then 45 cycles of 95°C 10s, 60°C 20s, 72°C 19s, followed by melt curve analysis. Primers: *HRPT*, forward primer: 5' ATTGACACTGGCAAAACAATGC 3', reverse primer: 5' TCCAACACTTCGTGGGGTCC 3', reference. *DRD4*, forward primer: 5' GTGGTGGTCGGGGCCTT 3' , reverse primer: 5' CGGAGCAGGCAGGACAC 3'. *DRD4* CT values were normalized to *HRPT* expression and *DRD4* relative gene expression vs untreated calculated.

Phospho-kinase Array

Primary human chondrocytes were seeded at 5 x 10^6 cells (2 x 10 cm adherent dish, Corning) in growth media and allowed to adhere overnight. Growth media was replaced with chondrogenic media supplemented with 1ng/mL TGFβ1 with DMSO or with aromoline (5μM). Cells were treated for 24 h before processing according to the manufacturer's protocol (ARY003C, R&D Systems). This phospho-kinase array contains capture antibodies to measure relative levels of phosphorylation of 37 kinases on a nitrocellulose membrane. Signal intensity was quantified using ImageJ using the Microarray Profile plug-in.

Statistical Analysis

Statistical analysis for all experiments was performed using GraphPad Prism 9 and volcano plot, multiple t-test with 1% false detection rate, one-way or two-way ANOVA with Dunnett's correction performed. All data passed tests for normality. In all figures * indicates p-value < 0.05, ** indicates p- value <0.01, and *** indicates p- value < 0.001.

References

1. USBJI. (Rosemont, IL, 2014), vol. 2022.
2. A. Carbone, S. Rodeo, Review of current understanding of post-traumatic osteoarthritis resulting from sports injuries. *J Orthop Res* **35**, 397-405 (2017).
3. W. Zhang, H. Ouyang, C. R. Dass, J. Xu, Current research on pharmacologic and regenerative therapies for osteoarthritis. *Bone Research* **4**, 15040 (2016).
4. E. B. Hunziker, K. Lippuner, M. J. B. Keel, N. Shintani, An educational review of cartilage repair: precepts & practice – myths & misconceptions – progress & prospects. *Osteoarthritis and Cartilage* **23**, 334-350 (2015).
5. A. P. Hollander *et al.*, Increased damage to type II collagen in osteoarthritic articular cartilage detected by a new immunoassay. *The Journal of Clinical Investigation* **93**, 1722-1732 (1994).
6. R. Stoop *et al.*, Type II collagen degradation in spontaneous osteoarthritis in C57BL/6 and BALB/c mice. *Arthritis & Rheumatism* **42**, 2381-2389 (1999).
7. A. J. Sophia Fox, A. Bedi, S. A. Rodeo, The Basic Science of Articular Cartilage: Structure, Composition, and Function. *Sports Health* **1**, 461-468 (2009).
8. G. A. Whitney, K. Jayaraman, J. E. Dennis, J. M. Mansour, Scaffold-free cartilage subjected to frictional shear stress demonstrates damage by cracking and surface peeling. *Journal of Tissue Engineering and Regenerative Medicine* **11**, 412-424 (2017).
9. G. A. Whitney *et al.*, Thyroxine Increases Collagen Type II Expression and Accumulation in Scaffold-Free Tissue-Engineered Articular Cartilage. *Tissue Engineering Part A* **24**, 369-381 (2017).
10. J. E. Dennis, T. Splawn, T. J. Kean, High-Throughput, Temporal and Dose Dependent, Effect of Vitamins and Minerals on Chondrogenesis. *Frontiers in Cell and Developmental Biology* **8**, (2020).
11. K. Sato, H. Mera, S. Wakitani, M. Takagi, Effect of epigallocatechin-3-gallate on the increase in type II collagen accumulation in cartilage-like MSC sheets. *Bioscience, Biotechnology, and Biochemistry* **81**, 1241-1245 (2017).
12. C. D. Hoemann, in *Cartilage and Osteoarthritis: Volume 2: Structure and In Vivo Analysis,* F. De Ceuninck, M. Sabatini, P. Pastoureau, Eds. (Humana Press, Totowa, NJ, 2004), pp. 127-156.
13. K. Martyniak *et al.*, Biomaterial composition and stiffness as decisive properties of 3D bioprinted constructs for type II collagen stimulation. *Acta Biomaterialia* **152**, 221-234 (2022).
14. M. A. Cruz *et al.*, Micronutrient Optimization Using Design of Experiments Approach in Tissue Engineered Articular Cartilage for Production of Type II Collagen. *bioRxiv*, 2022.2012.2007.519522 (2022).
15. A. P. Chidgey, D. Layton, A. Trounson, R. L. Boyd, Tolerance strategies for stem-cell-based therapies. *Nature* **453**, 330-337 (2008).
16. A. G. Atanasov *et al.*, Natural products in drug discovery: advances and opportunities. *Nature Reviews Drug Discovery* **20**, 200-216 (2021).
17. H. Lachance, S. Wetzel, K. Kumar, H. Waldmann, Charting, Navigating, and Populating Natural Product Chemical Space for Drug Discovery. *Journal of Medicinal Chemistry* **55**, 5989-6001 (2012).
18. G. M. Cragg, D. J. Newman, Natural products: A continuing source of novel drug leads. *Biochimica et Biophysica Acta (BBA) - General Subjects* **1830**, 3670-3695 (2013).
19. D. J. Newman, G. M. Cragg, Natural Products As Sources of New Drugs over the 30 Years from 1981 to 2010. *Journal of Natural Products* **75**, 311-335 (2012).
20. C. J. Henrich, J. A. Beutler, Matching the power of high throughput screening to the chemical diversity of natural products. *Natural Product Reports* **30**, 1284-1298 (2013).
21. J. G. Moffat, F. Vincent, J. A. Lee, J. Eder, M. Prunotto, Opportunities and challenges in phenotypic drug discovery: an industry perspective. *Nature Reviews Drug Discovery* **16**, 531-543 (2017).
22. J. E. Dennis, T. Splawn, T. J. Kean, High-Throughput, Temporal and Dose Dependent, Effect of Vitamins and Minerals on Chondrogenesis. *Frontiers in Cell and Developmental Biology* **8**, (2020).
23. J. E. Dennis, G. A. Whitney, J. Rai, R. J. Fernandes, T. J. Kean, Physioxia Stimulates Extracellular Matrix Deposition and Increases Mechanical Properties of Human Chondrocyte-Derived Tissue-Engineered Cartilage. *Frontiers in Bioengineering and Biotechnology* **8**, (2020).
24. A. Daina, O. Michielin, V. Zoete, SwissADME: a free web tool to evaluate pharmacokinetics, drug-likeness and medicinal chemistry friendliness of small molecules. *Scientific Reports* **7**, 42717 (2017).
25. A. Daina, O. Michielin, V. Zoete, SwissTargetPrediction: updated data and new features for efficient prediction of protein targets of small molecules. *Nucleic Acids Res* **47**, W357-W364 (2019).

26. D. Gfeller *et al.*, SwissTargetPrediction: a web server for target prediction of bioactive small molecules. *Nucleic Acids Research* **42**, W32-W38 (2014).
27. T. J. Kean, Z. Ge, Y. Li, R. Chen, J. E. Dennis, Transcriptome-Wide Analysis of Human Chondrocyte Expansion on Synoviocyte Matrix. *Cells* **8**, 85 (2019).
28. N. P. T. Huynh, B. Zhang, F. Guilak, High-depth transcriptomic profiling reveals the temporal gene signature of human mesenchymal stem cells during chondrogenesis. *The FASEB Journal* **33**, 358-372 (2019).
29. T. J. Kean, J. E. Dennis, Synoviocyte Derived-Extracellular Matrix Enhances Human Articular Chondrocyte Proliferation and Maintains Re-Differentiation Capacity at Both Low and Atmospheric Oxygen Tensions. *PLOS ONE* **10**, e0129961 (2015).
30. M. Pei, F. He, Extracellular matrix deposited by synovium-derived stem cells delays replicative senescent chondrocyte dedifferentiation and enhances redifferentiation. *Journal of Cellular Physiology* **227**, 2163-2174 (2012).
31. C. Jensen, Y. Teng, Is It Time to Start Transitioning From 2D to 3D Cell Culture? *Front Mol Biosci* **7**, 33 (2020).
32. W. M. Oo, C. Little, V. Duong, D. J. Hunter, The Development of Disease-Modifying Therapies for Osteoarthritis (DMOADs): The Evidence to Date. *Drug Des Devel Ther* **15**, 2921-2945 (2021).
33. F. Yano *et al.*, A novel disease-modifying osteoarthritis drug candidate targeting Runx1. *Ann Rheum Dis* **72**, 748-753 (2013).
34. L. G. Griffith, M. A. Swartz, Capturing complex 3D tissue physiology in vitro. *Nature Reviews Molecular Cell Biology* **7**, 211-224 (2006).
35. N. C. Foster, N. M. Hall, A. J. E. Haj, Two-Dimensional and Three-Dimensional Cartilage Model Platforms for Drug Evaluation and High-Throughput Screening Assays. *Tissue engineering. Part B, Reviews* **28**, 421-436 (2022).
36. C.-H. Hsieh, Y.-D. Chen, S.-F. Huang, H.-M. Wang, M.-H. Wu, The Effect of Primary Cancer Cell Culture Models on the Results of Drug Chemosensitivity Assays: The Application of Perfusion Microbioreactor System as Cell Culture Vessel. *BioMed Research International* **2015**, 470283 (2015).
37. A. A. Bulysheva, G. L. Bowlin, S. P. Petrova, W. A. Yeudall, Enhanced chemoresistance of squamous carcinoma cells grown in 3D cryogenic electrospun scaffolds. *Biomedical Materials* **8**, 055009 (2013).
38. Y. Sugimoto, Y. Sugimura, Y. Yamada, Production of bisbenzylisoquinoline alkaloids in cultured roots of Stephania cepharantha. *Phytochemistry* **27**, 1379-1381 (1988).
39. Y. Sugimoto, Y. Sugimura, Y. Yamada, Biosynthesis of bisbenzylisoquinoline alkaloids in cultured roots of Stephania cepharantha. *FEBS Letters* **273**, 82-86 (1990).
40. C. Weber, T. Opatz, in *The Alkaloids: Chemistry and Biology,* H.-J. Knölker, Ed. (Academic Press, 2019), vol. 81, pp. 1-114.
41. A. Hostalkova *et al.*, Isoquinoline Alkaloids from Berberis vulgaris as Potential Lead Compounds for the Treatment of Alzheimer's Disease. *Journal of Natural Products* **82**, 239-248 (2019).
42. C. K. Angerhofer, H. Guinaudeau, V. Wongpanich, J. M. Pezzuto, G. A. Cordell, Antiplasmodial and Cytotoxic Activity of Natural Bisbenzylisoquinoline Alkaloids. *Journal of Natural Products* **62**, 59-66 (1999).
43. D. Koutova *et al.*, Bersavine: A Novel Bisbenzylisoquinoline Alkaloid with Cytotoxic, Antiproliferative and Apoptosis-Inducing Effects on Human Leukemic Cells. *Molecules*. 2020 (10.3390/molecules25040964).
44. L. T. Ng, L.-C. Chiang, Y.-T. Lin, C.-C. Lin, Antiproliferative and Apoptotic Effects of Tetrandrine on Different Human Hepatoma Cell Lines. *The American Journal of Chinese Medicine* **34**, 125-135 (2006).
45. J. Wang, Y. Dong, Q. Li, Neferine induces mitochondrial dysfunction to exert anti-proliferative and anti-invasive activities on retinoblastoma. *Experimental Biology and Medicine* **245**, 1385-1394 (2020).
46. M. Rogosnitzky, P. Okediji, I. Koman, Cepharanthine: a review of the antiviral potential of a Japanese-approved alopecia drug in COVID-19. *Pharmacological reports : PR* **72**, 1509-1516 (2020).
47. M. Hristova, R. Istatkova, Complement-mediated antiinflammatory effect of bisbenzylisoquinoline alkaloid fangchinoline. *Phytomedicine* **6**, 357-362 (1999).
48. X. Wu, Y. Guo, X. Min, L. Pei, X. Chen, Neferine, a Bisbenzylisoquinoline Alkaloid, Ameliorates Dextran Sulfate Sodium-Induced Ulcerative Colitis. *The American Journal of Chinese Medicine* **46**, 1263-1279 (2018).
49. C. Missale, S. R. Nash, S. W. Robinson, M. Jaber, M. G. Caron, Dopamine Receptors: From Structure to Function. *Physiological Reviews* **78**, 189-225 (1998).

50. M. Jaber, S. W. Robinson, C. Missale, M. G. Caron, Dopamine receptors and brain function. *Neuropharmacology* **35**, 1503-1519 (1996).
51. M. Kawano, R. Takagi, K. Saika, M. Matsui, S. Matsushita, Dopamine regulates cytokine secretion during innate and adaptive immune responses. *International Immunology* **30**, 591-606 (2018).
52. F. McKenna *et al.*, Dopamine receptor expression on human T- and B-lymphocytes, monocytes, neutrophils, eosinophils and NK cells: a flow cytometric study. *Journal of Neuroimmunology* **132**, 34-40 (2002).
53. K. L. O'Malley, S. Harmon, L. Tang, R. D. Todd, The rat dopamine D4 receptor: sequence, gene structure, and demonstration of expression in the cardiovascular system. *The New biologist* **4**, 137-146 (1992).
54. P. A. Jose *et al.*, The renal dopamine receptors. *Journal of the American Society of Nephrology* **2**, (1992).
55. R. H. McDonald, Jr., L. I. Goldberg, J. L. McNay, E. P. Tuttle, Jr., Effects of Dopamine in Man: Augmentation of Sodium Excretion, Glomerular Filtration Rate, and Renal Plasma Flow. *The Journal of Clinical Investigation* **43**, 1116-1124 (1964).
56. R. Pivonello *et al.*, Dopamine Receptor Expression and Function in Human Normal Adrenal Gland and Adrenal Tumors. *The Journal of Clinical Endocrinology & Metabolism* **89**, 4493-4502 (2004).
57. M. B. Murphy, Dopamine: a role in the pathogenesis and treatment of hypertension. *Journal of Human Hypertension* **14**, S47-S50 (2000).
58. D. E. Hernandez, G. A. Mason, C. H. Walker, J. E. Valenzuela, Dopamine receptors in human gastrointestinal mucosa. *Life Sciences* **41**, 2717-2723 (1987).
59. J. A. Schuurkes, J. M. Van Nueten, Domperidone improves myogenically transmitted antroduodenal coordination by blocking dopaminergic receptor sites. *Scandinavian journal of gastroenterology. Supplement* **96**, 101-110 (1984).
60. J. W. Kebabian, Dopamine-sensitive adenylyl cyclase: a receptor mechanism for dopamine. *Adv Biochem Psychopharmacol* **19**, 131-154 (1978).
61. J. W. Kebabian, D. B. Calne, Multiple receptors for dopamine. *Nature* **277**, 93-96 (1979).
62. L. Tang, R. D. Todd, A. Heller, K. L. O'Malley, Pharmacological and functional characterization of D2, D3 and D4 dopamine receptors in fibroblast and dopaminergic cell lines. *J Pharmacol Exp Ther* **268**, 495-502 (1994).
63. P. M. van der Kraan, E. N. Blaney Davidson, A. Blom, W. B. van den Berg, TGF-beta signaling in chondrocyte terminal differentiation and osteoarthritis: modulation and integration of signaling pathways through receptor-Smads. *Osteoarthritis Cartilage* **17**, 1539-1545 (2009).
64. F. Beier, R. F. Loeser, Biology and pathology of Rho GTPase, PI-3 kinase-Akt, and MAP kinase signaling pathways in chondrocytes. *J Cell Biochem* **110**, 573-580 (2010).
65. B. Costanza, I. A. Umelo, J. Bellier, V. Castronovo, A. Turtoi, Stromal Modulators of TGF-beta in Cancer. *J Clin Med* **6**, (2017).
66. J.-M. Beaulieu *et al.*, An Akt/Beta-Arrestin 2/PP2A Signaling Complex Mediates Dopaminergic Neurotransmission and Behavior. *Cell* **122**, 261-273 (2005).
67. J.-M. Beaulieu, T. Del' Guidice, T. Sotnikova, M. Lemasson, R. Gainetdinov, Beyond cAMP: The Regulation of Akt and GSK3 by Dopamine Receptors. *Frontiers in Molecular Neuroscience* **4**, (2011).
68. R. L. Miclea *et al.*, Inhibition of Gsk3β in cartilage induces osteoarthritic features through activation of the canonical Wnt signaling pathway. *Osteoarthritis Cartilage* **19**, 1363-1372 (2011).
69. S. Guidotti *et al.*, Glycogen Synthase Kinase-3β Inhibition Links Mitochondrial Dysfunction, Extracellular Matrix Remodelling and Terminal Differentiation in Chondrocytes. *Scientific reports* **7**, 12059-12059 (2017).
70. Y. Kawasaki *et al.*, Phosphorylation of GSK-3beta by cGMP-dependent protein kinase II promotes hypertrophic differentiation of murine chondrocytes. *J Clin Invest* **118**, 2506-2515 (2008).
71. S. Guidotti *et al.*, Lithium Chloride Dependent Glycogen Synthase Kinase 3 Inactivation Links Oxidative DNA Damage, Hypertrophy and Senescence in Human Articular Chondrocytes and Reproduces Chondrocyte Phenotype of Obese Osteoarthritis Patients. *PLoS One* **10**, e0143865 (2015).
72. E. M. Rosethorne, S. J. Charlton, Agonist-Biased Signaling at the Histamine H4 Receptor: JNJ7777120 Recruits β-Arrestin without Activating G Proteins. *Molecular Pharmacology* **79**, 749 (2011).
73. M. T. Drake *et al.*, Beta Arrestin-biased Agonism at the Beta 2 Adrenergic Receptor *. *Journal of Biological Chemistry* **283**, 5669-5676 (2008).
74. J. D. Violin, R. J. Lefkowitz, β-Arrestin-biased ligands at seven-transmembrane receptors. *Trends in Pharmacological Sciences* **28**, 416-422 (2007).

75. B. Masri *et al.*, Antagonism of dopamine D2 receptor/beta-arrestin 2 interaction is a common property of clinically effective antipsychotics. *Proc Natl Acad Sci U S A* **105**, 13656-13661 (2008).
76. J. A. Allen *et al.*, Discovery of β-Arrestin–Biased Dopamine D2 Ligands for Probing Signal Transduction Pathways Essential for Antipsychotic Efficacy. *Proceedings of the National Academy of Sciences* **108**, 18488-18493 (2011).
77. Y. Jin *et al.*, A novel prostaglandin E receptor 4 (EP4) small molecule antagonist induces articular cartilage regeneration. *Cell Discov* **8**, 24 (2022).
78. D. Lennon, S. Haynesworth, S. Bruder, N. Jaiswal, A. Caplan, Human and animal mesenchymal progenitor cells from bone marrow: Identification of serum for optimal selection and proliferation. *In Vitro Cellular & Developmental Biology - Animal* **32**, 602-611 (1996).
79. J. E. Dennis, G. A. Whitney, J. Rai, R. J. Fernandes, T. J. Kean, Physioxia Stimulates Extracellular Matrix Deposition and Increases Mechanical Properties of Human Chondrocyte-Derived Tissue-Engineered Cartilage. *Frontiers in Bioengineering and Biotechnology* **8**, (2020).
80. T. J. Kean *et al.*, Disparate response of articular- and auricular-derived chondrocytes to oxygen tension. *Connect Tissue Res* **57**, 319-333 (2016).
81. W. Boehmler *et al.*, D4 Dopamine receptor genes of zebrafish and effects of the antipsychotic clozapine on larval swimming behaviour. *Genes Brain Behav* **6**, 155-166 (2007).
82. C. Sarkar *et al.*, Cutting Edge: Stimulation of dopamine D4 receptors induce T cell quiescence by up-regulating Kruppel-like factor-2 expression through inhibition of ERK1/ERK2 phosphorylation. *J Immunol* **177**, 7525-7529 (2006).
83. S. Dolma *et al.*, Inhibition of Dopamine Receptor D4 Impedes Autophagic Flux, Proliferation, and Survival of Glioblastoma Stem Cells. *Cancer Cell* **29**, 859-873 (2016).
84. R. D. Truong, M. A. Bernier, J. E. Dennis, T. J. Kean, Synoviocyte-Derived Extracellular Matrix and bFGF Speed Human Chondrocyte Proliferation While Maintaining Differentiation Potential. *Frontiers in Bioengineering and Biotechnology* **10**, (2022).
85. R. W. Farndale, C. A. Sayers, A. J. Barrett, A direct spectrophotometric microassay for sulfated glycosaminoglycans in cartilage cultures. *Connect Tissue Res* **9**, 247-248 (1982).

Acknowledgments: The plasmids, pMD2.G, and psPAX2, were a gift from Didier Trono (Addgene plasmid # 12259; http://n2t.net/addgene:12259; RRID:Addgene_12259) and (Addgene plasmid # 12260; http://n2t.net/addgene:12260; RRID:Addgene_12260) respectively. The type II collagen antibody, II-II6B3 was deposited to the DSHB by Linsenmayer, T.F. (DSHB Hybridoma Product II-II6B3).

Funding:

Rolanette and Berdon Lawrence Bone Disease Program of Texas (TJK)
University of Central Florida (TJK)
University of Central Florida College of Medicine (TJK).

Author contributions: Each author's contribution(s) to the paper should be listed [we encourage you to follow the CRediT model]. Each CRediT role should have its own line, and there should not be any punctuation in the initials.

Examples:
Conceptualization: MAC, TJK
Methodology: MAC, TJK
Software: MAC, RM, TJK
Investigation: MAC, MK, KM, RM, TJK
Visualization: MAC, TJK
Funding acquisition: TJK
Project administration: TJK

Supervision: MAC, TJK
Writing – original draft: MAC
Writing – review & editing: MAC, TJK

Competing interests: A patent application on "Anabolic Drugs Stimulating Type II Collagen Production from Chondrocytes or their Progenitors" is pending.

Data and materials availability: All data, code, and materials used in the analysis must be available in some form to any researcher for purposes of reproducing or extending the analysis. Include a note explaining any restrictions on materials, such as materials transfer agreements (MTAs). Note accession numbers to any data relating to the paper and deposited in a public database; include a brief description of the data set or model with the number. If all data are in the paper and supplementary materials, include the sentence "All data are available in the main text or the supplementary materials."

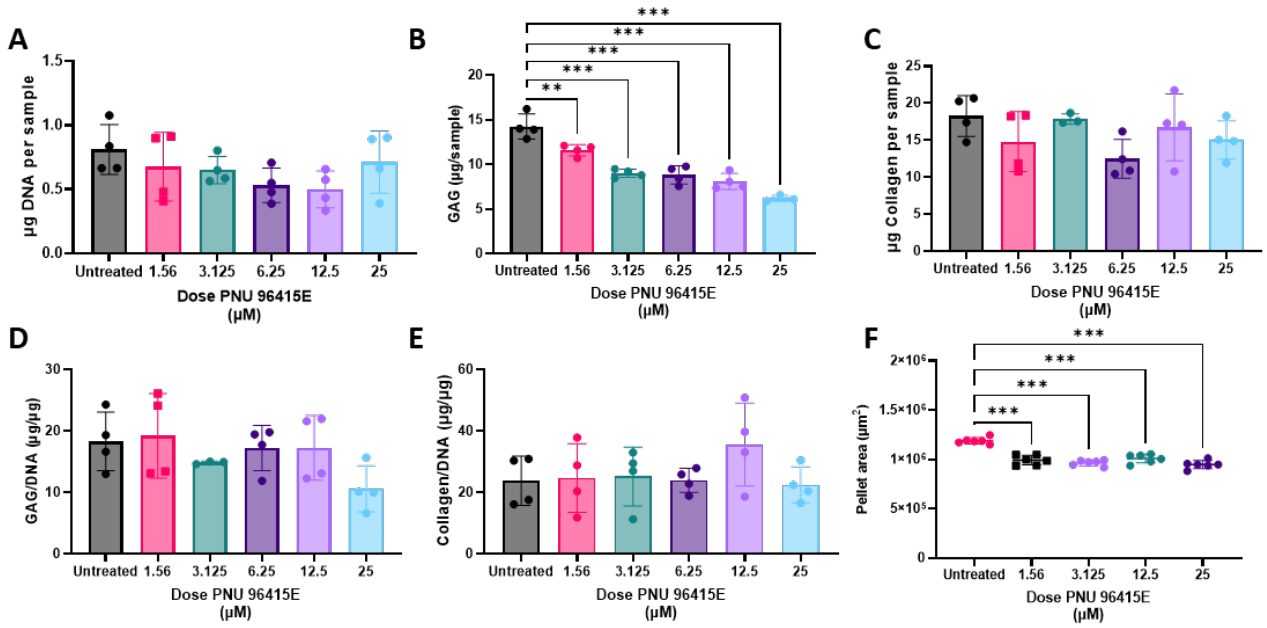

Supplemental Figure 1. DRD4 antagonist effect on cartilage aggregate biochemistry

Aggregate DNA (**A**), glycosminoglycan (**B)** and collagen content (**C**) are shown from aggregates treated with the DRD4 antagonist PNU 96415E (0-25 µM). The relative concentrations of GAG/DNA (**D**) and collagen/DNA (**E**) and aggregate size (**F**) are shown. N ≥ 4. Individual replicates or mean of replicates are shown with error bars indicating standard deviation and ** indicating p <0.01, and *** indicating p <0.001 vs. untreated control.

SwissTargetPrediction	Sum of probability
Dopamine D2 receptor (by homology)	2.851672
Dopamine D1 receptor	2.137331
Neuronal acetylcholine receptor; alpha4/beta2	1.985921
Dopamine D3 receptor	1.749336
Serotonin 1a (5-HT1a) receptor	1.587394
Serotonin 7 (5-HT7) receptor	1.511987
Mu opioid receptor	1.377361
Serotonin 2a (5-HT2a) receptor	1.291214
P-glycoprotein 1	1.27206
Acetylcholinesterase	1.074565
Serotonin 6 (5-HT6) receptor	1.049648
Serotonin 2b (5-HT2b) receptor	1.041349
Dopamine transporter	1.029377
Adenosine A2b receptor	1
Protein tyrosine phosphatase receptor type C-associated protein	0.955943
Serotonin transporter	0.893932
Neuronal acetylcholine receptor; alpha3/beta4	0.880203
Dopamine D4 receptor	0.865448
Dopamine transporter (by homology)	0.84436
HERG	0.830416
Serotonin 5a (5-HT5a) receptor	0.785328
Alpha-1a adrenergic receptor (by homology)	0.707984
Multidrug and toxin extrusion protein 1	0.705785
Dopamine D5 receptor	0.693454
Serotonin 2c (5-HT2c) receptor	0.656597
Alpha-1d adrenergic receptor	0.639058
Adrenergic receptor alpha-2	0.636835
Alpha-2a adrenergic receptor	0.636835
Alpha-2b adrenergic receptor	0.636835
Beta-1 adrenergic receptor	0.630121
Serotonin 1d (5-HT1d) receptor	0.612378
Butyrylcholinesterase	0.612333
Alpha-1b adrenergic receptor	0.590313
Rho-associated protein kinase 2	0.560261
Adrenergic receptor beta	0.541904
Serotonin 1b (5-HT1b) receptor	0.532355
Serine/threonine-protein kinase AKT	0.52625
Cyclin-dependent kinase 2/cyclin A	0.467339
Serotonin 3a (5-HT3a) receptor	0.467339
Tyrosine-protein kinase JAK2	0.467339
Dipeptidyl peptidase IV	0.459682
Histamine H2 receptor	0.451933
Tyrosine-protein kinase SRC	0.444029
Indoleamine 2,3-dioxygenase	0.421457
Rho-associated protein kinase 1	0.421457
Delta opioid receptor	0.4031